



Study Effect of Central Rectangular Perforation on the Natural Convection Heat Transfer in an Inclined Heated Flat Plate

Lect. Kadhum Audaa Jehhef

Department of Equipment and Machine
Institute of Technology, Middle Technical University
Email: kadhum.audaa@yahoo.com

ABSTRACT

A numerical solutions is presented to investigate the effect of inclination angle (θ), perforation ratio (m) and wall temperature of the plate (T_w) on the heat transfer in natural convection from isothermal square flat plate up surface heated (with and without concentrated hole). The flat plate with dimensions of (128 mm) length \times (64 mm) width has been used five with square models of the flat plate that gave a rectangular perforation of ($m=0.03, 0.06, 0.13, 0.25, 0.5$). The values of angle of inclination were ($0^\circ, 15^\circ, 30^\circ, 45^\circ, 60^\circ$) from horizontal position and the values of wall temperature ($50^\circ\text{C}, 60^\circ\text{C}, 70^\circ\text{C}, 90^\circ\text{C}, 100^\circ\text{C}$). To investigate the temperature, boundary layer thickness and heat flux distributions; the numerical computation is carried out using a very efficient integral method to solve the governing equation. The results show increase in the temperature gradient with increase in the angle of inclination and the high gradient and high heat transfer coefficients located in the external edges of the plate, for both cases: with and without holed plate. There are two separation regions of heat transfer in the external edge and the internal edges. The boundary layer thickness is small in the external edge and high in the center of the plate and it decreases as the inclination angle of plate increases. Theoretical results are compared with previous result and it is found that the Nusslet numbers in the present study are higher by (22 %) than that in the previous studies. And the results show good agreement in range of Raleigh number from 10^5 to 10^6 .

Key words: natural convection, perforation plate, inclined flat plate.

دراسة تأثير تجويف مستطيل مركزي على انتقال الحرارة بالحمل الحراري الحر فوق صفيحة مائلة مسخنة

م.د. كاظم عودة جحف

قسم المكين والمعدات

معهد تكنولوجيا- بغداد , الجامعة التقنية الوسطى

الخلاصة

قدمت دراسة عددية لاستقصاء تأثير زاوية الميل (θ) ونسبة التجويف (m) ودرجة حرارة السطح (T_w) على انتقال الحرارة بالحمل الحر من صفيحة مستوية مربعة مسخنة من الوجه الاعلى (مع وبدون تجويف مركزي) والصفيحة بطول (128 ملم) وسماك (64 ملم) وتم استخدام خمس نماذج للصفيحة المربعة مع ثقوب مستطيل ذات نسب تجويف مختلفة هي ($m=0.03, 0.06, 0.13, 0.25, 0.5$) وبزاويا ميل مختلفة هي ($0^\circ, 15^\circ, 30^\circ, 45^\circ, 60^\circ$) من الوضع الافقي وقيم درجات حرارة متغيرة تتضمن ($50^\circ\text{C}, 60^\circ\text{C}, 70^\circ\text{C}, 90^\circ\text{C}, 100^\circ\text{C}$) ومن اجل دراسة توزيع كلا من درجة الحرارة وسمك الطبقة المتاخمة والفيض الحراري باستخدام التحليل العددي بطريقة التكامل لحل المعادلات الرياضية الحاكمة. اظهرت النتائج ان هناك زيادة في انحدار درجات الحرارة مع زيادة زاوية الميل للصفيحة. ويتمركز اعلى انحدار في درجات حرارة واعلى قيمة لمعامل انتقال الحرارة في الحافات الخارجية للصفيحة لكنتا الحالتين (مع وبدون تجويف). وهناك منطقتي انفصال لانتقال الحرارة تتمركز في الحافات الداخلية والخارجية للصفيحة المجوفة. ولوحظ ان سمك الطبقة المتاخمة الحرارية يكون قليل في الحافة الخارجية وعالي في مركز الصفيحة في حالة النموذج الخالي من تجويف. وتبدأ هذه الطبقة بالتناقص كلما ازدادت زاوية الميلان وتمت



مقارنة النتائج النظرية الحالية مع نتائج سابقة وجد ان اعداد نسلت في البحث الحالي اعلى بنسبة (22%) عما موجود في البحوث السابقة ووجد تقارب جيد بين النتائج في مدي رقم رالي من 10^5 الى 10^6 .
الكلمات الرئيسية: الحمل الحر، صفيحة مثقبة، صفيحة مستوية مائلة.

1. INTRODUCTION

Natural convection cooling of components in electronics which has been attached to printed circuit boards, which are placed vertically and horizontally in an enclosure, is currently of great interest to the microelectronics industry. Natural convection cooling is desirable because it doesn't require energy source, such as a forcing by fan and it is maintenance free and safe. Cavities with no obstructions were studied in the past few years such as **Zhong et. al., 1985** and **Saravanan and Kandaswamy, 2000**. The exact solutions available in the literature, especially that was related to the boundary layer thickness and temperature profiles and showed that there was a limited attention to study the effect of the perforation in the flat plate.

The heat transfer by natural convection applied to simple geometries such as flat plates, spheres, and cylinders, has been extensively studied for decades. **Ostrach, 1952**, was one who of those solves the boundary layer equations for natural convection from vertical flat plate using a numerical method. The set of three equations a continuity, momentum and energy were reduced to only two equations with their respective boundary conditions. He found that this type of flow was dependent on the Grashof number and Prandtl number.

The geometry of an inclined, semi infinite without holed flat plates had been considered by a number of researchers because of its engineering applications. Among whom are **Ganesan and Palani, 2003**, **Said et. al., 2005**, **Sparrow and Husar, 1969** and **Patterson, et. al. 2007**. Most of these studies had been conducted by either numerical simulations or experimental observations. **Zekeriya and kurtul, 2006**, performed a numerical study of laminar natural convection in tilted rectangular enclosures that contain a vertically situated hot plate using the finite volume method with SIMPLE algorithm. The Raleigh number and the tilt angle of the enclosure were ranged from 10^5 to 10^7 and from 0° to 90° respectively. **Kobus and Wedekind 2000**, presented experimental heat transfer data and developed dimensionless correlation for natural convection from heated horizontal stationery isothermal circular disks over a wide range of Raleigh numbers. The air was used with variety of disks of different diameters and thickness-to-diameters aspect ratios. Another type of important convective heat transfer problem is the free and mixed convection boundary-layer flow near a flat plate which is inclined at a small arbitrary angle to the horizontal or vertical plate. **Jones, 1973** studied theoretically the free convection boundary-layer near a flat plate at small angles of inclinations to the horizontal by taking into account both the parallel and the normal to the plate temperature gradients which drive the fluid flow and both positive and negative inclination angles of the plate were considered. When the inclination angles of the plate was positive, both of the mechanisms which drive the flow produce favorable effective pressure gradients, so that the fluid continued to be accelerated along the plate to a final state, far from the leading edge, which was described by the classical free convection boundary-layer solution over a vertical flat plate. For negative inclination angles, although the pressure gradient associated with the processes remained



favorable, separation of the boundary-layer from the plate eventually occurred, since the buoyancy force opposes the motion. Important contributions to these convective flow configurations had also been made by several authors, notably by **Schneider, 1995**, **Umemura and Law, 1990**, **Weidman and Amberg, 1996** and **Waheed, 2001**, conducted a numerical study to solve the governing equation with the finite difference volume method for the disks and rings with outer diameter ($0.2 \leq r_1 \leq 0.9$) (where r_1 is the ratio of inner to outer diameter) heated from the upper surface with constant temperature in range of Grashof number ($10^3 \leq Gr_{Do} \leq 10^7$). He observed that the main process of heat transfer was conduction at Grashof number less than (10^3) and the convection at Grashof number less than (10^3). The maximum rate of heat transfer for the rings that had the same outer diameter for the disk was achieved at the inner diameter with outer diameter between (0.2-0.3).

Mohammed, 2002, studied experimentally the laminar heat transfer by natural convection from the disks. **Waheed, 2001**, used inclined upward and downward heated rings at constant temperature in the range of Raleigh number ($1.7 \times 10^5 \leq Ra_{Do} \leq 3.1 \times 10^6$). The results showed that the average Nusselt number which depended wholly on the angle of inclination, and there was clear difference in the rates of heat transfer between the horizontal upward and downward surfaces where the effect of inner diameter was limited to the increase which leads to rates of heat transfer in the case of upward rings. Addition of the extended surface to the external edge leads to decrease in the rates of heat transfer for all inclination angles. **Abd, 2005**, presented a numerical study of three dimensional laminar natural convection heat transfer process from isothermal square plate and another plate with a circular perforation (ratio of perforation to the plate external length ranges from 0.6 to 0.8), and angle of inclination ranging from (0° - 180°). The numerical study included solution of the momentum and energy equations by using the finite difference method for the range of Grashof number ($10^3 \leq Gr_{Do} \leq 5 \times 10^4$) with Prandtle number ($Pr=0.72$). The results showed that the maximum temperature gradient was achieved at external edge for the case of horizontal perforation square plate and heated from upward and at lower external edge for the case of inclination plate. The local Nusselt number for the perforation plate wholly depended on the inclination angles and the values of average Nusselt number with a higher level than the square plate and increase as the perforation ratio increase. While the values of average Nusselt number increases with increasing of the inclination angles for the upward heated square plate and reach the high limit at the vertical position, then decrease the inclination angles. **Kadhim, 2003**, studied three dimensional natural convection heat transfer from the rings and disks (inner to outer diameter equal to 0.2, 0.5 and 0.8) angles of inclination ranged from ($0^\circ \leq \theta \leq 180^\circ$) with Prandtle number ($Pr=0.72$). The results showed that the local Nusselt number wholly depends on the inclination angles. The variation in inner diameter caused a limited increase in the heat transfer rates in case of the heated upward rings and high effected in case of rings heated downward. The average Nusselt number increases with the increase in the angle of inclination and the ratio of inner to outer diameter for heated upward rings. Where the maximum value of average Nusselt number is in depended of the inclination angles, its change depends only on the inner to outer diameter ratio for these rings. The maim aim of this study is investigating the enhancement the shared influence of the plate perforation and angle inclination

on the natural convection heat transfer process by using the numerical computation carried out using the integral method to solve the governing equation and compare the theoretical result with those of the previous studies.

2. PHYSICAL MODELS AND MATHEMATICAL FORMULATION

Consider the steady free convection flow of a viscous incompressible fluid over an inclined semi-infinite plate at an angle (θ), as shown in **Fig. 1**. The temperature of plate is assumed constant at (T_w) and the ambient fluid has the uniform temperature T_∞ , where $T_w > T_\infty$. For this configuration, the assumption is that the Boussinesq approximation is valid, **Ioan 2001**.

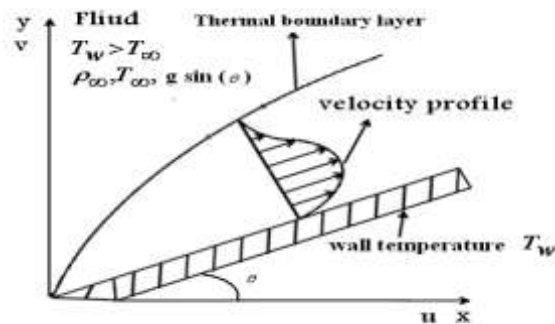


Figure 1. Physical models and coordinate systems of the heated inclined flat plate.

The body force by unit volume is $-\rho g \sin(\theta)$, where g is the local acceleration of gravity. And the key assumptions are:

- 1) Constant properties (ρ , k , C_p), except for the variation in density that drives the flow
- 2) Pressure gradients perpendicular to the plate can be neglected.
- 3) Density variation can be approximated by a linear dependence on temperature. This is called the Boussinesq approximation.
- 4) Diffusive transport (of both momentum and energy) in the direction parallel to the plate can be neglected. There are also, of course, many other implied assumptions (steady-state situation, viscous dissipation is negligible in the energy equation, everything is constant in the z -direction (parallel to plate, perpendicular to gravity)).

First, will be look up the “general” governing equations in a reference text, to find the following equations. Any terms involving the z coordinate or the corresponding velocity component, can be neglected as well as the transient terms. This leaves: **Rolando, 2004**, the basic conservation Eqs. (1), (2) and (3) can be written as follows:

Continuity equation (overall mass balance)

$$u \frac{\partial(\rho u)}{\partial x} + v \frac{\partial(\rho u)}{\partial y} = 0 \quad (1)$$

and momentum balance in x direction (parallel to plate and gravity) for a Newtonian fluid with constant ρ and μ .



$$\rho \left[\frac{\partial u}{\partial t} + u \frac{\partial u}{\partial x} + v \frac{\partial u}{\partial y} \right] = -\frac{\partial P}{\partial x} + \eta \left[\frac{\partial^2 u}{\partial x^2} + \frac{\partial^2 u}{\partial y^2} \right] - \rho g \sin(\theta) \quad (2)$$

For a horizontal flat plate, the energy balance for a Newtonian fluid with constant ρ and μ equation reduces to,

$$u \frac{\partial T}{\partial x} + v \frac{\partial T}{\partial y} = \alpha \frac{\partial^2 T}{\partial y^2} \quad (3)$$

where

$$\left[\frac{\partial u}{\partial t} \right] = \mathbf{0}$$

$$\frac{\partial^2 u}{\partial x^2} \ll \frac{\partial^2 u}{\partial y^2}$$

Then, Eq. (2) becomes:

$$\rho \left[u \frac{\partial u}{\partial x} + v \frac{\partial u}{\partial y} \right] = -\frac{\partial P}{\partial x} + \eta \left[\frac{\partial^2 u}{\partial y^2} \right] - \rho g \sin(\theta) \quad (4)$$

$$\frac{\partial P}{\partial x} = -\rho_{\infty} g \sin \theta \quad (5)$$

where ρ_{∞} is the density outside the boundary layer. Replacing Eq. (5) in Eq. (4) yields

$$\rho \left[u \frac{\partial u}{\partial x} + v \frac{\partial u}{\partial y} \right] = g \sin(\theta)(\rho_{\infty} - \rho) + \eta \left[\frac{\partial^2 u}{\partial y^2} \right] \quad (6)$$

The first term on the right-hand side of Eq. (6) is the buoyancy force, where the density ρ is a variable. The density may be represented by a linear function of temperature for small temperature differences and the change in density is related to the thermal expansion, β , as: **Rolando, 2004**,

$$\beta = -\frac{1}{\rho} \left(\frac{\partial \rho}{\partial T} \right)_p \quad (7)$$

If β is approximated by:

$$\beta \cong -\frac{1}{\rho} \left(\frac{\rho_{\infty} - \rho}{T_{\infty} - T} \right) \quad (8)$$

then

$$\rho_{\infty} - \rho \cong \rho \beta (T - T_{\infty}) \quad (9)$$

and Eq. (2) becomes, **Rolando, 2004**:

$$u \frac{\partial u}{\partial x} + v \frac{\partial u}{\partial y} = g(\sin \theta) \beta (T - T_{\infty}) + \gamma \frac{\partial^2 u}{\partial y^2} \quad (10)$$

hence, the buoyancy force is related to the temperature difference.



Momentum integral method is approximate and much easier to apply to a wide range of problems than any exact method of solution. The idea behind this: is it is not really interest in the detailing of the velocity or temperature profiles beyond learning their slopes at the wall (**John, 2004**). [These slopes give the shear stress at the wall is $\tau_w = \mu(\partial u/\partial y)_{y=0}$ and the heat flux at the wall is $q_w = k(\partial T/\partial y)_{y=0}$ **Schlichting, 1979**, where the boundary conditions are:

$$\begin{aligned} T &= T_w & \text{at } y = 0 \\ T &= T_\infty & \text{for } y \gg \infty \\ u &= v = 0 & \text{at } y = 0 \\ u &= v = 0 & \text{for } y \gg \infty \end{aligned}$$

If the integral method is applied in Eqs. (10 and 3), these equations (momentum and energy equations) will be respectively, **John, 2004**:

$$\frac{d}{dx} \int_0^\delta u^2 dy \cong g\beta \int_0^\delta (T - T_\infty) dy - \nu \left. \frac{\partial u}{\partial y} \right|_{y=0} \quad (11)$$

$$\frac{d}{dx} \int_0^\delta u(T - T_\infty) dy \cong -\alpha \left. \frac{\partial T}{\partial y} \right|_{y=0} \quad (12)$$

The functional forms are assumed as follows, **John, 2004**

$$u = u_1 \xi (1 - \xi)^2 \quad (13)$$

and

$$\phi = \frac{T - T_\infty}{T_w - T_\infty} = (1 - \xi)^2 \quad (14)$$

The first derivative of this equation with respect to (y) will be, **John, 2004**

$$\left. \frac{\partial T}{\partial y} \right|_{y=0} = -\frac{2}{\delta} (T_w - T_\infty) \quad (15)$$

where $\xi = \frac{y}{\delta}$

After the first derivative of Eq. (13) is used and equaled to zero in order to obtain the value of maximum velocity component termed u_1 substituting this equation with Eq. (15) into Eq. (11) gives the general solution of the laminar thermal boundary layer without pressure gradient

$$\frac{\delta}{x} = 3.93 [0.952 + pr]^{\frac{1}{4}} (pr)^{-\frac{1}{2}} (Gr_x)^{-\frac{1}{4}} \quad (16)$$

the Gr_x is the local Grashof number

$$Gr_x = \frac{g \sin(\theta) \beta (T_w - T_\infty) x^3}{\nu^2}$$

where (θ) is the inclination angle of flat plate with horizontal position.

The solution of the boundary-layer equations for any convection heat transfer problem gives the velocity and temperature distributions. This is true for any type of solution (analytical or numerical) and for any type of convection (forced or natural). Once the solution is obtained, the heat-transfer coefficient is obtained by realizing that as we approach the solid surface, the velocity vector is tangent to the surface and the heat-flux vector is normal to the surface, thus the heat transfer is by conduction at the limit as the distance from the wall approaches zero. Therefore, for the problem described in the previous section, the heat flux is:

$$q = h(T_w - T_\infty) = k \left. \frac{\partial T}{\partial y} \right|_{y=0} \quad (17)$$

Subtracting into Eq. (17), will give:

$$\frac{h}{k} = \frac{2}{\delta}$$

The value of δ from Eq. (16) is used to get the local heat transfer coefficient along the length of flat plate with respect to x component as follows:

$$h_x = 0.508(pr)^{\frac{1}{2}} [0.952 + pr]^{\frac{1}{4}} k (Gr_x)^{\frac{1}{4}} x^{-\frac{1}{4}} \quad (18)$$

The Nusselt number is found from the following relation:

$$Nu_x = \frac{h_x x}{k} \quad (19)$$

The heat dissipation from the heated flat plate can be determined from the following relation:

$$Q = hA(T - T_w) \quad (20)$$

3. PROBLEM DEFINITION

In natural or free convective heat transfer, heat is transferred between a solid surface and a fluid moving over it, where the fluid motion is entirely caused by the buoyancy forces arising from density changes that result from the temperature variations in the fluid, this motion is called natural convection which can be either laminar or turbulent. However, because of the low velocities that usually exist in natural convection, laminar flow occurs more frequently than turbulent flow. In this paper, attention is therefore focused on two dimensional laminar natural convective flow. If the temperature differences are small enough, the fluid properties, except the fluid density, may be assumed to be constant (fluid density can not be assumed constant, because its variation induces the fluid motion).

In the present work a heated aluminum flat plate is used with dimensions of (128mm length \times 64mm width) and additionally five models of central perforation are used heated from upward flat plate with dimension of rectangular perforates dimensions of (2mm \times 4mm), (4mm \times 8mm), (8mm \times 16mm), (16mm \times 32mm) and (32mm \times 64mm) are represented by the ratio of the flat plate length to the perforation length of (m=0.03, 0.06, 0.13, 0.25 and 0.5) respectively. The constant wall temperatures used in this search were (50°C, 60 °C, 70 °C, 90 °C, 100 °C). **Fig. 2** illustrates the flat plate with and without central perforation and shows the perforation length.

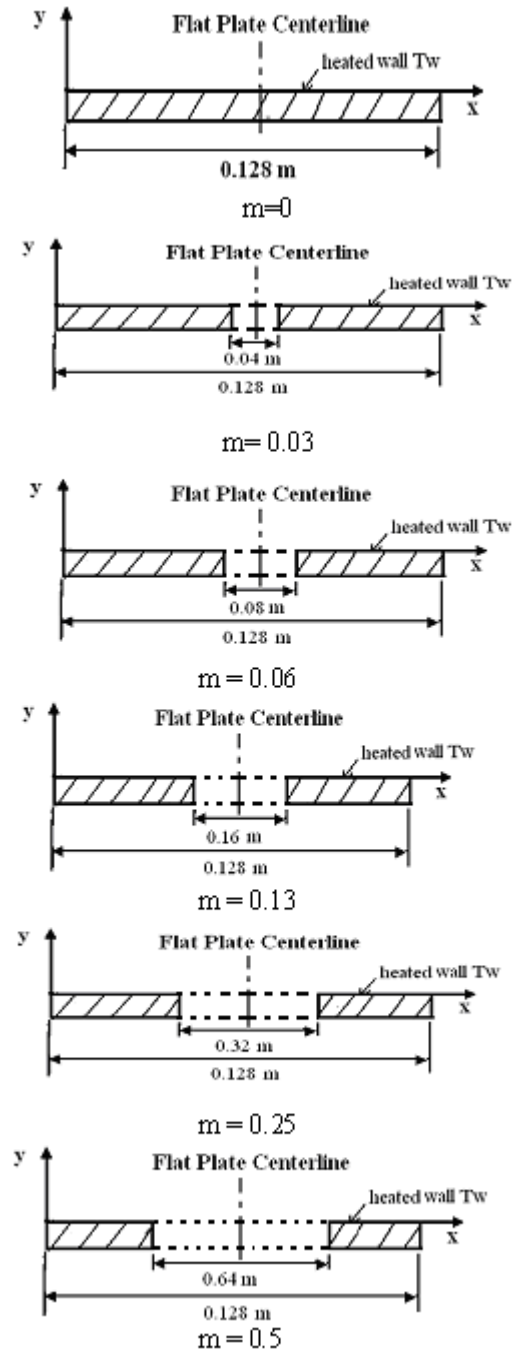


Figure 2. The studied models of flat plate have been heated from upward surface.

4. RESULTS AND DISCUSSION

The figures in this paper were generated by the (MATLAB 7) simulation program to study the effect of the five central rectangular perforations in the heated upward flat plate. **Figs. 3 and 4** show the relationship between the distribution of dimensionless wall temperatures gradient and the region above the flat plate represented by y-direction for the model of heated upward rectangle flat plate without perforation ($m=0$) for values along the x-direction ranging as follows ($x/L_o = 1, 0.75, 0.5, 0.25, 0.15, 0.06$ and 0.03) at horizontal position ($\theta=0^\circ$). The results compared with the results of the model ($m=0.13$) for range of values along the x-direction ($x/L_o = 1, 0.75, 0.5, 0.25$) at the same position ($\theta=0^\circ$). The numerical data shows that central perforation is used in the plate in order to avoid entering the slight declination region. The temperature gradients were located at positions ($x/L_o = 0.03, 0.06$ and 0.15) in the range of the central perforation. The figures show that high temperatures gradient along y-direction is achieved for the all models at the external edge while the low temperatures gradient exists at the internal edge of perforation models and increases with increasing the perforation ratio. And **Fig. 5** shows the development of the thermal boundary layer thickness (δ) along the x-direction of the heated flat plate for various value of the wall temperature ($50^\circ\text{C}, 60^\circ\text{C}, 70^\circ\text{C}, 90^\circ\text{C}, 100^\circ\text{C}$) for two selected models of ($m=0$ and 0.13) respectively at horizontal position ($\theta=0^\circ$). As is shown in these figures, the thermal boundary layer thickness (δ) is low at the external edge and increases gradually towards the flat plate center, because the fluid molecular density near the models edges is higher than that near the center with high velocity leading to generate the Plume (the thermal separation happens). As a result the thermal boundary layer thickness (δ) increases at the center more than at edges. The transmitted heat at the thermal separation region will be less than that at the external edge.

Fig. 6 shows the development of thermal boundary layer along x-axis for various values of wall temperature for the model of heated flat plate ($m= 0.13$). It is noticed that the thickness of thermal boundary layer increases gradually from the edge of flat plate towards the center and decreases as the wall temperature increases. in comparison with the model ($m= 0.13$) in **Fig.5** which shows in that the thickness of boundary layer is interrupted in the edge at ($x=0.056$ m) while in the centerline of flat plate at ($x=0.064$ m), the boundary layer thickness increases from the external edges towered the internal edge in which the thickness decreases with increase in the perforation ratio, compared with first model ($m=0$) show that the thickness of boundary layer decreases with increasing the perforation ratio because of the increase in the temperature gradient at the internal edges.

Figs. 7 and 8 present the effect of flat plate inclination angle on the thermal boundary layer thickness for two models of the heated plate ($m= 0$) and ($m= 0.13$). As shown in these figures, the thermal boundary layer decreases as the angle inclination deviates from horizontal towards inclined

position because increasing the temperatures gradient, **Abd 2005**. Eventually; the effect of all models of upward heated flat plate on the dimensionless wall temperature gradients (ϕ) with y -direction are collected in **Fig. 9** that shows the increasing the dimension of the central perforation from ($m=0$ and 0.06) leads to increasing the dimensionless wall temperature gradients, then this increase goes down when the model ($m=0.5$) is used because the high area removed from the flat plate leading to decreasing the wall temperature distribution exposed to the ambient.

The local heat transfer coefficient h_{Lo} at horizontal position ($\theta=0^\circ$) of two models of heated plate ($m=0$) and ($m=0.13$) is shown in **Fig. 10** the maximum values are achieved in the external edge because of the movement of the thermal boundary layer, and the heat separation at this location of the flat plate. The local heat transfer coefficients decrease gradually from the edge of the flat plate towards the center and the minimum values are at centerline, where the local heat transfer coefficients increase as the wall temperatures increases. The effect of using perforation model of ($m=0.13$) shown in **Fig. 11**. There are two regions of the heat separation along the upper surface of heated flat plate: the first one exists in the external edge ($x=0$) of the plate because this edge is adjacent to the infinity medium and the second one at ($x=0.056$) near the perforation internal edge because this edge is adjacent to the finite medium. **Fig. 12** shows the effect of perforation ratio on the local Nusselt numbers for all models ($m=0, 0.03, 0.06, 0.13, 0.25$ and 0.5) with x -direction at horizontal position ($\theta=0^\circ$) the figure shows that the high value of local Nusselt numbers is located in the external edge of the heated flat plate and at perforation edge, The local Nusselt numbers increase as the perforation dimension increases and show that the model ($m=0.5$) shows high value of Nusselt numbers compared with other models.

Fig. 13 shows the relation between the logarithmic local Nusselt numbers with the algorithm of the local Raleigh numbers ($1.5 \times 10^5 \leq Ra_x \leq 6.3 \times 10^5$) at horizontal position ($\theta=0^\circ$), where the logarithmic local Nusselt numbers increase as the perforation ratio increases, because by using the perforation technique, the extraction of the thermal separation region centric in the central of the plate. And when the inclination angles increase to ($\theta=30^\circ$) as in **Fig. 14** the relation between the logarithm of the local Nusslet numbers and the algorithm of the local Raleigh numbers ($1.01 \times 10^5 \leq Ra_x \leq 6.4 \times 10^5$) for the all models, show that the local Nusslet numbers increase as the perforation dimensions and the angle of inclination increase, and the high local Nusselt numbers of ($Nu = 0.761 Ra^{0.201}$) of the model ($m=0$) and ($Nu = 0.985 Ra^{0.211}$) of the model ($m=0.13$) where the perforation dimensions are ($8\text{mm} \times 16\text{mm}$) at inclination of angle of (30°) and the increasing ratio between ($m=0$) and ($m=0.13$) is (23%) .

A comparison of average Nusselt numbers for the square plate in present study with those of the previous practical and numerical studies on the horizontal square heated plate for, **Abd 2005** illustrated in **Fig. 15** which shows the average Nusselt numbers for the present study at angle of inclination ($\theta = 0^\circ$) with no central perforation of model ($m=0$) increasing by (15 %). in the other



hand, the results are compared with those of the previous studies which used horizontal heated disk for **Abd, 2005**, **Mohammed, 2002** and **Kadhim, 2003** as shown in **Fig. 16** which shows that the average Nusselt numbers agreement with the value studied by them. And at Raleigh number 1.47×10^5 the model ($m=0.5$) shows that Nusselt numbers in the present study compared with those in the previous studies give an increase of about (20.3%), (22.6%) and (22.1 %) for the results of **Abd, 2005**, **Mohammed, 2002** and **Kadhim, 2003** respectively. This study show a good agreement in terms of the Nusselt numbers for the heated upward plate at angle of inclination ($\phi = 30^\circ$) with central perforation of model ($m=0.25$) compared with the square plate perforated with the circular perforation of **Abd, 2005** and rings of the, **Mohammed. 2002**.

6. CONCLUSIONS

A numerical investigation was carried out to study the natural convection heat transfer in the rectangular upward heated inclined perforated flat plate. In this paper, the influence of perforation ratio (m), Raleigh number (Ra), the angle of inclination (θ) and wall temperatures (T_w) were investigated. The numerical results show that: (1) the thermal boundary layer thickness increases as the wall temperature increases and as the angle of inclination decreases (2) The maximum values of local heat transfer coefficients are achieved at the leading edge of the flat plat for all models and at any angle of inclination. (3) The heat transfer process is enhanced with the perforation dimension increases. (4) The average Nusslet number for the present paper at angle of inclination ($\theta=0^\circ$) with no central perforated perforation ratio ($m=0$) increases by (15 %). (5) The Nusselt number values agree with these values presented by previous studies, with increase by (22 %) at ($Ra=1.47 \times 10^5$) and ($m=0.5$).

REFERENCES

- Abd Y.H. 2005, *Numerical study for a three dimensional laminar natural convection heat transfer from an isothermal heated horizontal and inclined square plate and with a circule hole*" M. Sc. Thesis University of Technology.
- Ioan, L. M. 2001, *Convective Heat Transfer: Mathematical and Computational Modeling of Viscous Fluids and Porous Media*. Elsevier Science & Technology Books.
- Ganesan, P. & Palani, G. 2003, *Natural convection effects on impulsively started inclined plate with heat and mass transfer*, Heat and Mass Transfer, 39, 277–283.
- Jones, D. R. 1973. *Free convection from a semi-infinite flat plate inclined at a small angle to the horizontal*. Q. J. Mech. Appl. Math. 26, 77-98.
- John H. Lienhard 2004, *A Heat Transfer Textbook*" Mechanical Engineering. University of Houston.



- Kobus G.L and Wedekind R.O. 2000 , *An experimental investigation into Natural convection heat transfer from horizontal stationary isothermal circular disks* Department of Mechanical Engineering, Oakland University 5 May.
- Kadhim A.H., 2003, *Prediction of three dimensional natural convection from heated disks and rings at constant temperature*. J. Eng. and Technology. Vol.22, No.5, pp.229-248.
- Mohammed J.A., 2002., *Measurement of three dimensional natural convection heat transfer from disks and rings facing upward and downward at constant temperature* M. Sc. Thesis University of Baghdad.
- Ostrach S., 1952. *An Analysis of Laminar Free-Convection Flow and Heat Transfer about a Flat Plate Parallel to the Direction of the Generating Body Force*. Report 1111-Supersedes NACA TN 2635.
- Patterson J.C, Lei C. and. Saha S.C. 2007. *On the Natural Convection Boundary Layer Adjacent to an Inclined Flat Plate Subject to Ramp Heating* School of Engineering James Cook University, Townsville, QLD 4811, Australia December.
- Umemura, A. and Law, C. K. 1990. *Natural Convection Boundary-Layer Flow Over a Heated Plate with Arbitrary Inclination*. J. Fluid Mech. 219, 571-584.
- Rolando A. Carrefio 2004, *Natural Convection Heat Transfer in Supercritical Fluid* Mechanical Engineering University of Puerto Rico.
- Saravanan S. and Kandaswamy P., 2000. *Natural Convection in low Prandtl number Fluids with a Vertical Magnetic Field*, ASME J. Heat Transfer, 122, pp. 602–606.
- Said, S. A. M., Habib, M. A., Badr, H. M. and Anwar, S. 2005. *Turbulent Natural Convection Between Inclined Isothermal Plates*, Computers & Fluid, 34, 1025–1039.
- Sparrow, E. M. and Husar, R. B., 1969. *Longitudinal Vortices in Natural Convection Flow on Inclined Plates* , J. Fluid. Mech.37, , 251–255.
- Schneider, W. 1995. *Laminar Mixed Convection Flows on Horizontal Surfaces*". In 3rd, Caribbean Congr. Fluid Dyn. Volume II, Simon Bolivar Univ., Caracas, pp. 1-7.
- Schlichting H., 1979. *Boundary Layer Theory*, seventh edition translated by Kestin J., McGraw-Hill Book Company , new york.
- Waheed A.M. 2001. *Numerical and Experimental Study Natural Convection Heat Transfer from Isothermal Horizontal Disks and Rings*. M. Sc. Thesis University of Technology
- Weidman, P. D. and Amberg, M. F. 1996. *Similarity Solutions for Steady Laminar Convection Along Heated Plates with Variable Oblique Suction*. Newtonian and Daxcian fluid flow. Q. J. Mech. Appl. Math. 49,373-403.
- Zhong Z.Y., Yang K. T., Lloyd J. R., 1985. *Variable Property Effects in Laminar Natural Convection in a Square Enclosure*, ASME J. Heat Transfer, 17, pp. 133–138.
- Zekeriya and kurtul 2006 *Natural Convection in Tilted Rectangular Enclosures with a Vertically Situated Hot Inside*" Osmangazi University 7 July.



NOMENCLATURES

A	area of the heated plate, m^2
Nu	average Nusselt number, --
p	pressure, N/m ²
g	acceleration due to gravity, m/s^2
t	dimensional time, s
Gr	Grashof number, ---
h	average heat transfer coefficient, $W/m^2 \cdot ^\circ C$
h_x	local heat transfer coefficient, $W/m^2 \cdot ^\circ C$
u, v	dimensional velocity components, m/s
x, y	dimensional coordinates, m
Nu_x	local Nusselt number, ---
Pr	Prandtl number, ---
m	perforation ratio, ---
k	thermal conductivity, $W/m \cdot ^\circ C$
T	predicted temperature
T_∞	ambient temperature
T_w	plate wall temperature
x	

Greek Symbols

α	thermal conductivity, m^2/s
β	volumetric coefficient of thermal expansion, 1/K
θ	angle of inclination, degree
ρ	density, kg/m^3
δ	boundary layer thickness, mm
ν	kinematic viscosity, m^2/s
μ	absolute viscosity, $kg/m \cdot s$
ϕ	dimensionless temperature
ζ	dimensionless viscosity

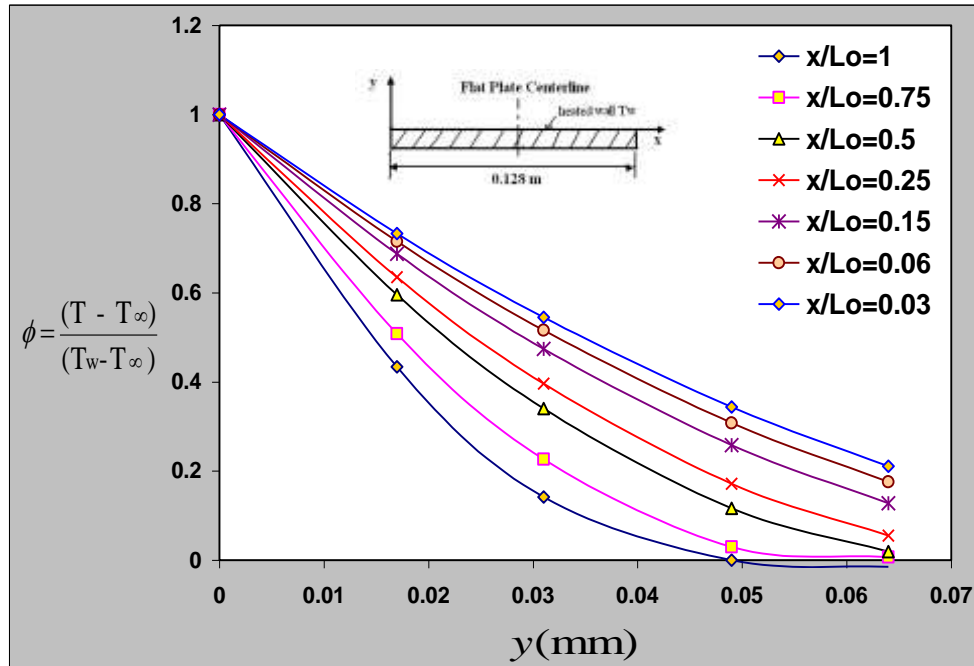


Figure 3. Dimensionless wall temperatures gradient vs. y -direction for the model of heated upward rectangle flat plate without perforation ($m=0$) for range values along the x -direction at horizontal position ($\theta=0^\circ$).

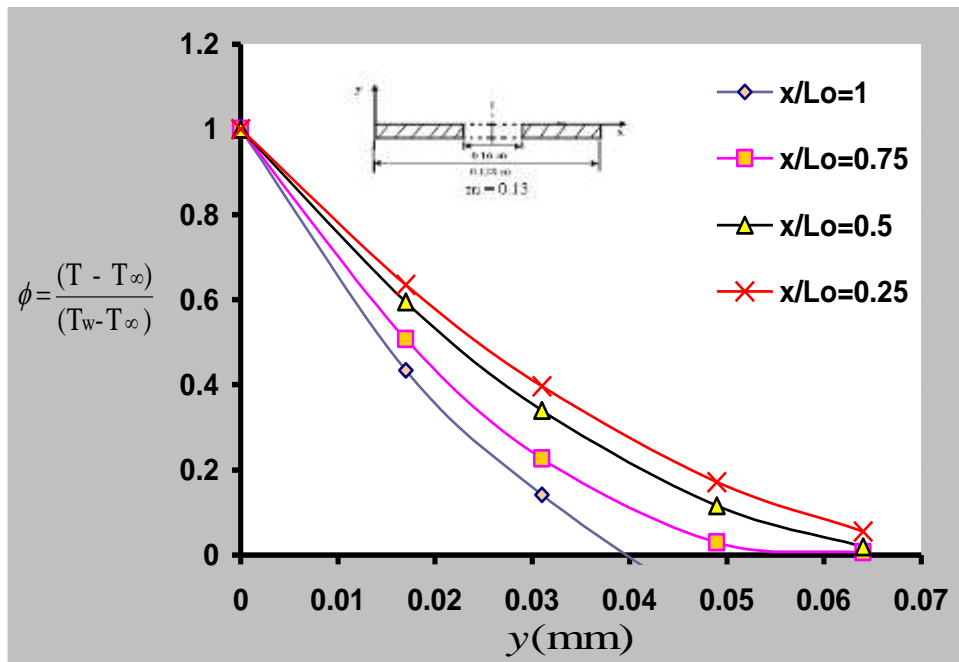


Figure 4. Dimensionless wall temperature gradients vs. y -direction for the model of heated upward rectangle flat plate with central perforation of dimension of $(16\text{mm} \times 32\text{mm})$ ($m=0.13$) for range values along the x -direction at horizontal position ($\theta=0^\circ$).

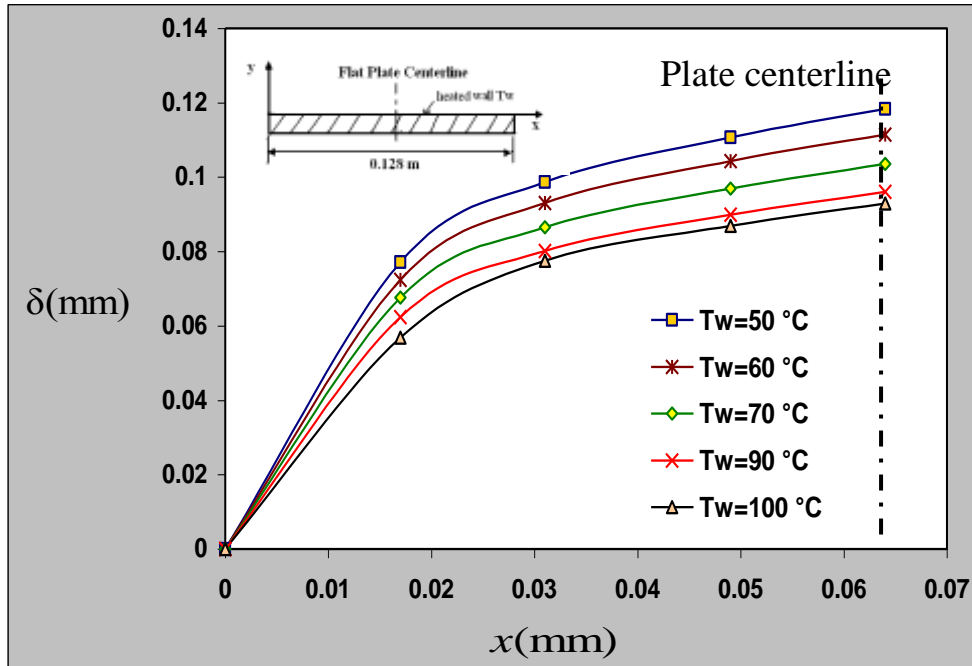


Figure 5. Thermal boundary layer thickness vs. x-direction for the model of heated upward rectangle flat plate without perforation ($m=0$) for a range of wall temperature.

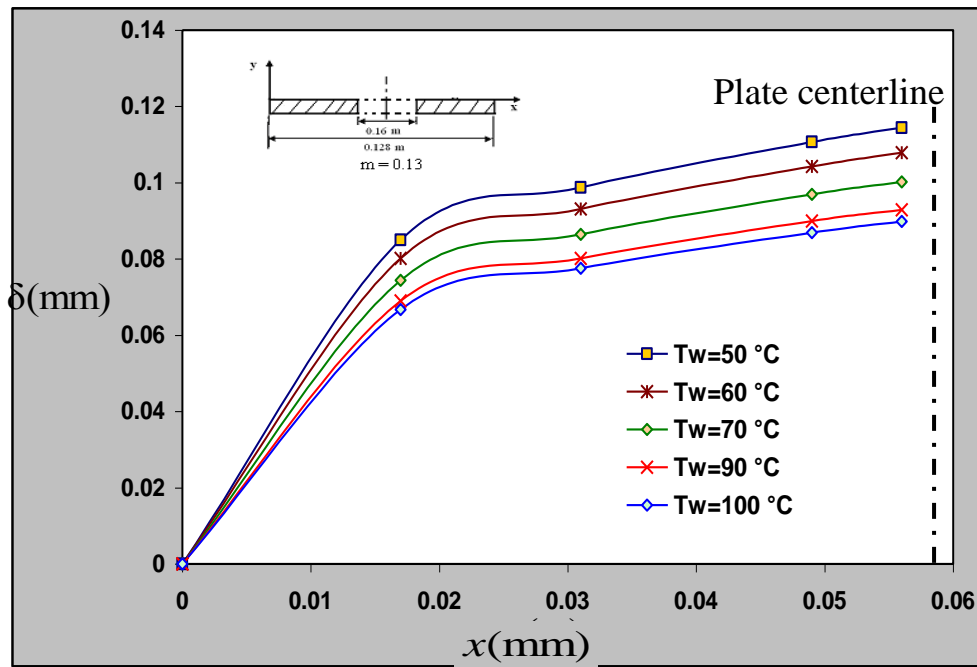


Figure 6. Thermal boundary layer thickness vs. x-direction for the model of heated upward rectangle flat plate with central perforation of dimensions (16mm×32mm) ($m=0.13$) for a range of wall temperature.

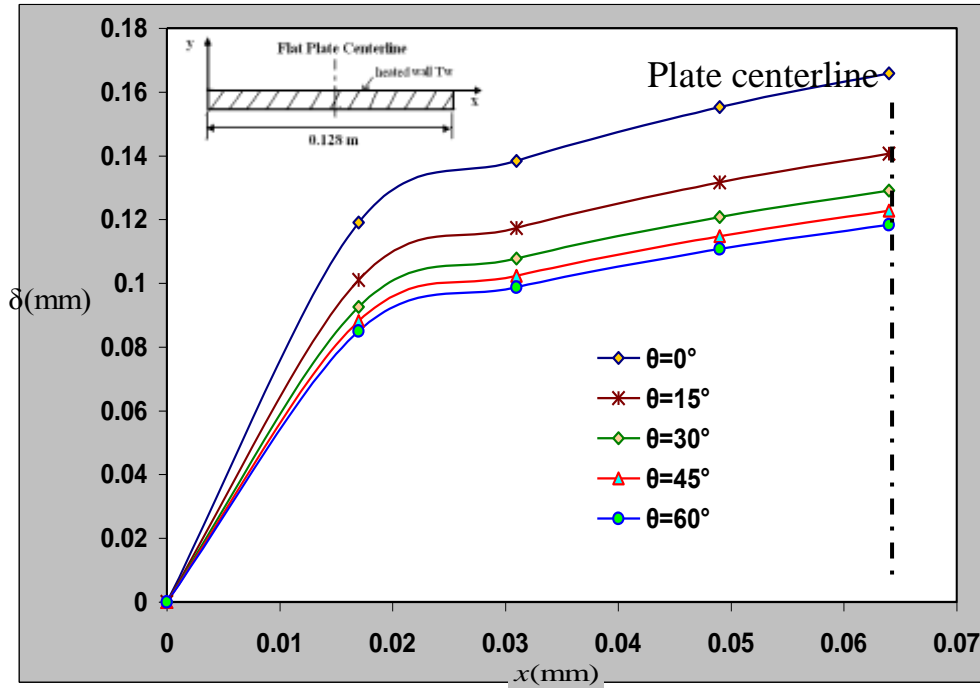


Figure 7. Thermal boundary layer thickness vs. x-direction for the model of heated upward rectangle flat plate without perforation ($m=0$) for a range of inclination angles.

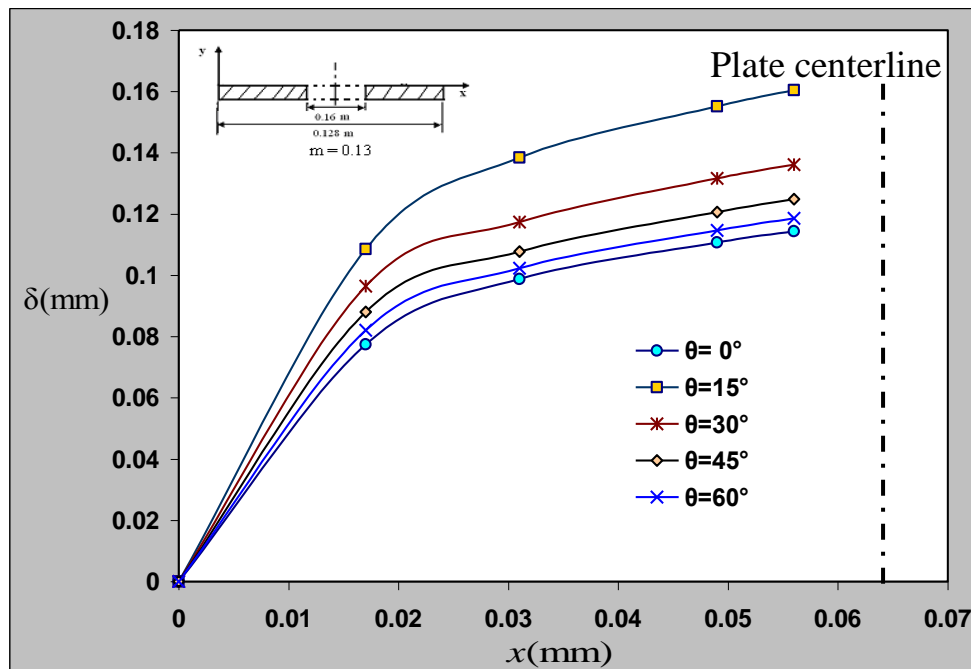


Figure 8. Thermal boundary layer thickness vs. x-direction for the model of heated upward rectangle flat plate with central perforation of dimensions (16mm \times 32mm) ($m=0.13$) for a range of inclination angles.

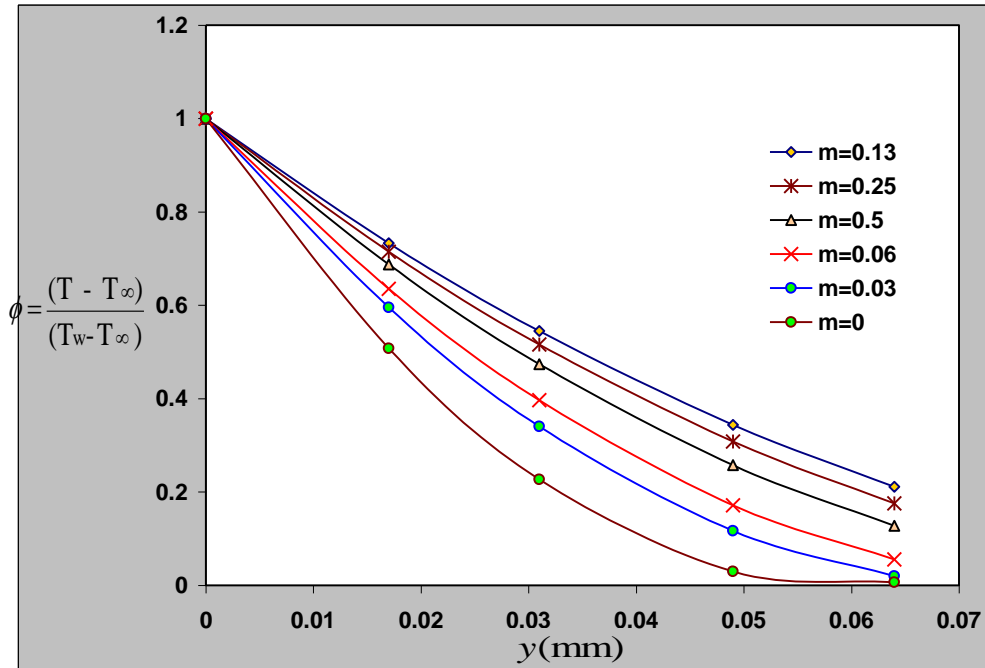


Figure 9. Dimensionless wall temperatures gradient vs. y-direction for the all studied models of heated upward rectangle flat plate.

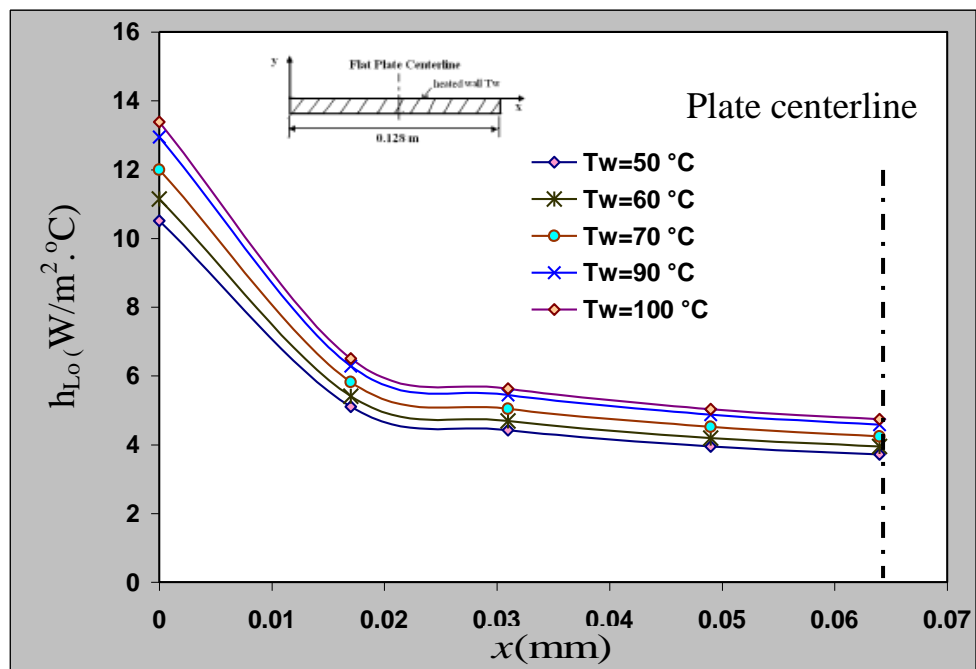


Figure 10. Local heat transfer coefficients vs. x-direction for the model of heated upward rectangle flat plate without perforation ($m=0$) for a range of wall temperature at horizontal position ($\theta=0^\circ$).

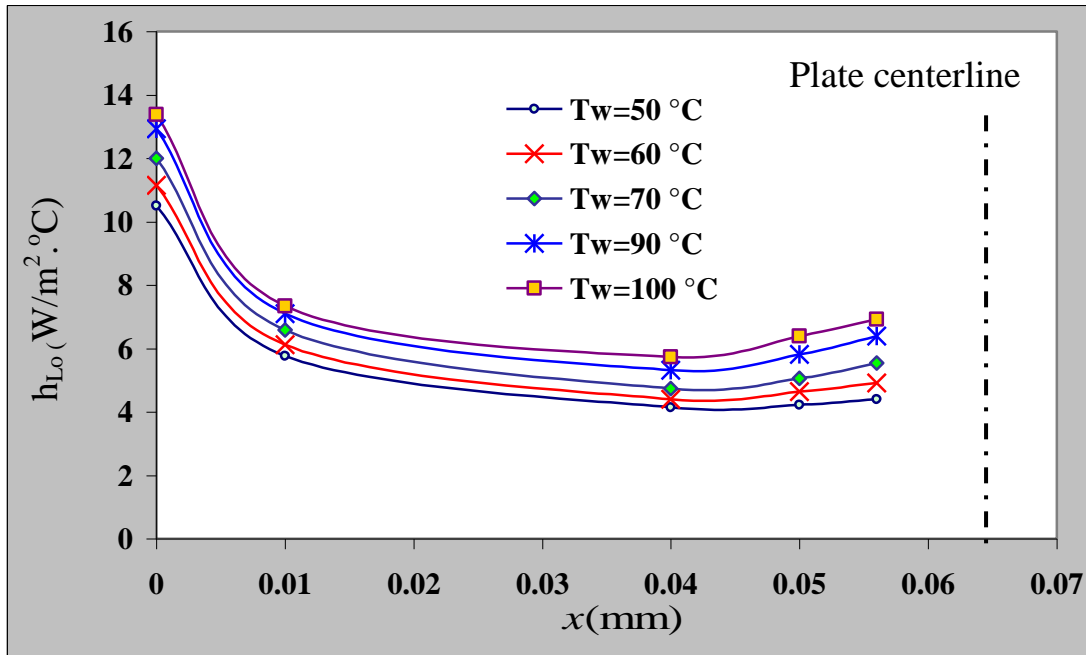


Figure 11. Local heat transfer coefficients vs. x-direction for the model of heated upward rectangle flat plate with central perforation of dimensions (16mm×32mm) ($m=0.13$) for a range of wall temperature at horizontal position ($\theta=0^\circ$).

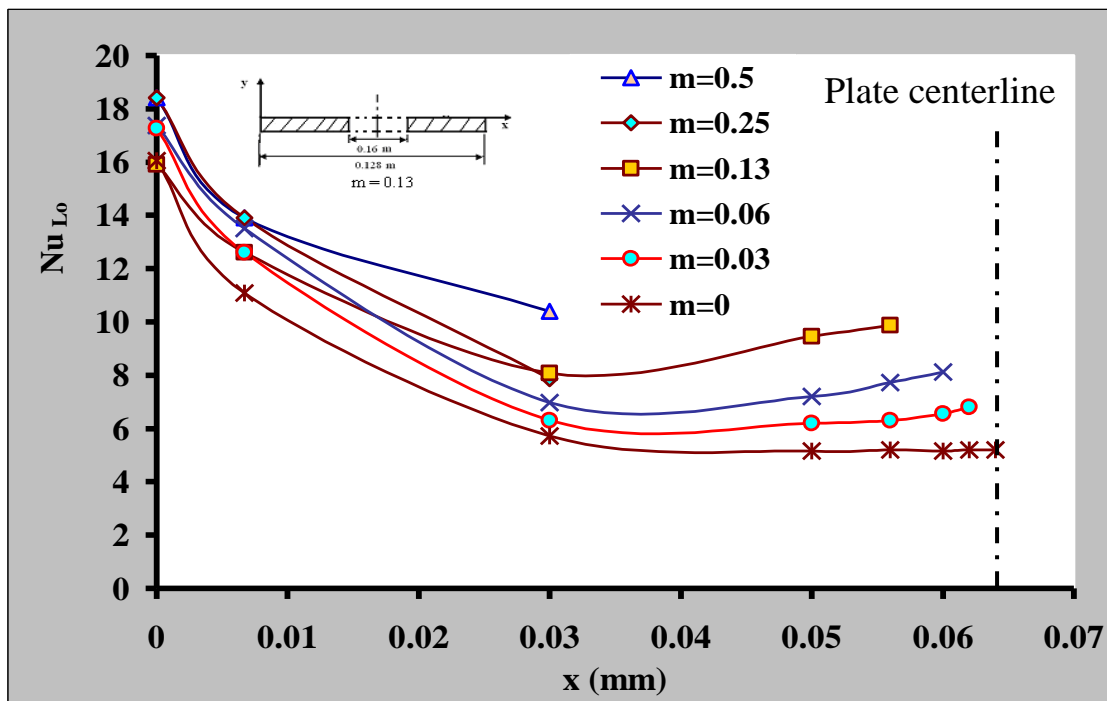


Figure 12. Comparison the distribution local Nusselt number vs. x-direction for all studied models of heated upward rectangle flat plate angle of inclination (0°).

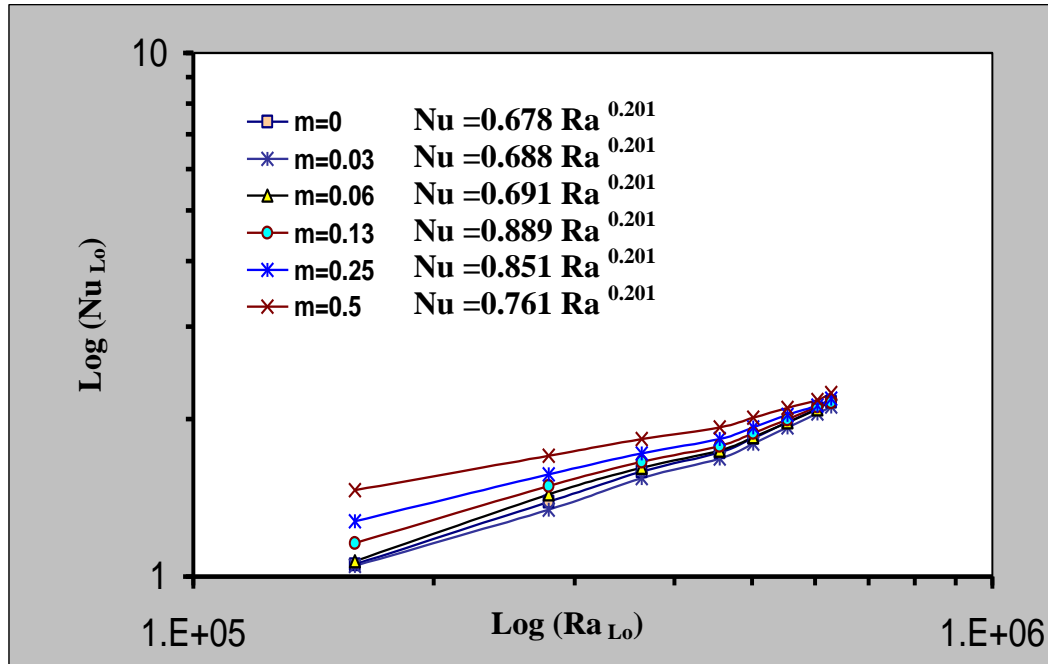


Figure 13. Comparison the distribution the local Nusselt number vs. Raleigh number for all studied models of heated upward rectangle flat plate for horizontal position at angle of inclination (0°)

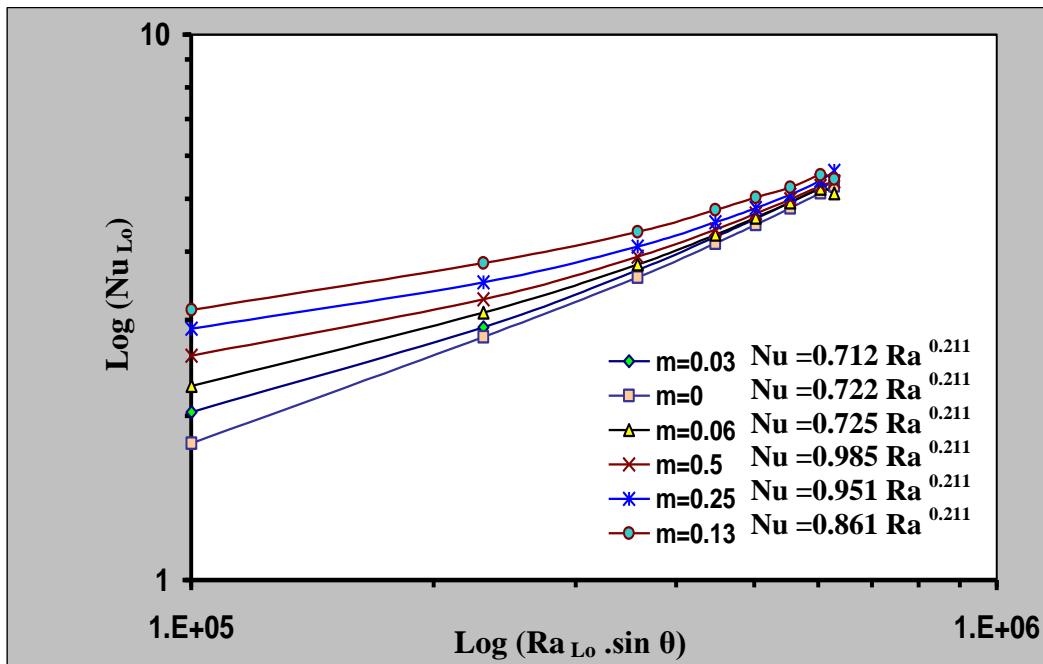


Figure 14. Comparison the distribution the local Nusselt number vs. Raleigh number for all studied models of heated upward rectangle flat plate for horizontal position at angle of inclination (30°).

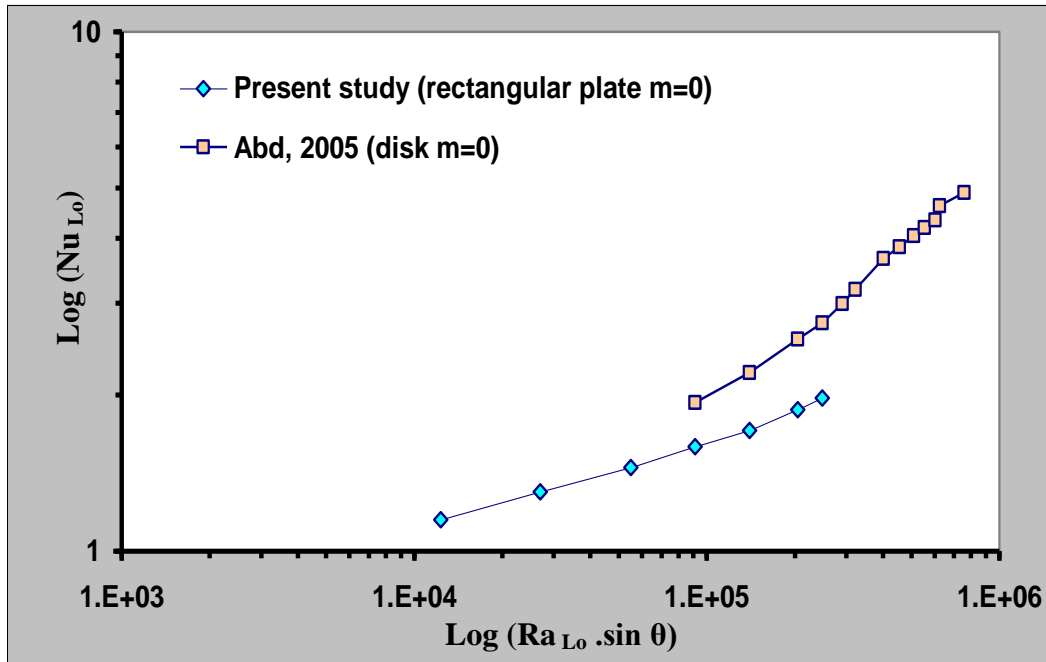


Figure 15. Comparison of the distributions of the logarithm Nusselt number vs. Raleigh number without perforation ($m=0$) heated upward rectangle flat plate for horizontal position at angle of inclination (0°).

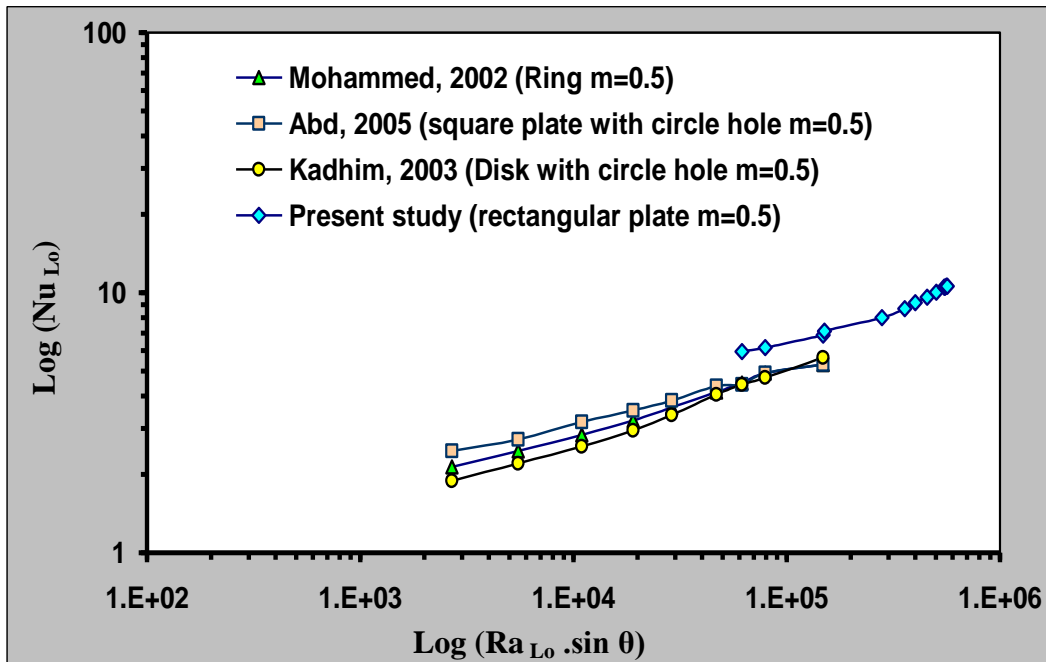


Figure 16. Comparison of the distribution of the local Nusselt number vs. Raleigh number with perforation ($m=0.5$) heated upward rectangle flat plate for horizontal position at angle of inclination (30°).